The Functional Influence of Breast Implant Outer Shell Morphology on Bacterial Attachment and Growth

Phoebe Jones, M.B.B.S.
Maria Mempin, B.Med.Sc., M.Res.(Med.)
Honghua Hu, Ph.D.
Durdana Chowdhury, M.B.B.S., M.Phil., Ph.D.
Matthew Foley, Ph.D.
Rodney Cooter, M.D.
William P. Adams, Jr., M.D.
Karen Vickery, B.V.Sc., Ph.D.
Anand K. Deva, B.Sc.(Med.), M.B.B.S., M.S.

Sydney, New South Wales, Australia; and Dallas, Texas

Background: The introduction of texture to the outer shell of breast implants was aimed at increasing tissue incorporation and reducing capsular contracture. It has also been shown that textured surfaces promote a higher growth of bacteria and are linked to the development of breast implant–associated anaplastic large cell lymphoma.
Methods: The authors aimed to measure the surface area and surface roughness of 11 available implants. In addition, the authors aimed to subject these implant shells to an in vitro bacterial attachment assay with four bacterial pathogens (*Staphylococcus epidermidis*, *S. aureus*, *Pseudomonas aeruginosa*, and *Ralstonia pickettii*) and study the relationship among surface area, surface roughness, and bacterial growth.
Results: Surface area measurement showed grouping of implants into high, intermediate, low, and minimal. Surface roughness showed a correlation with surface area. The in vitro assay showed a significant linear relationship between surface area and bacterial attachment/growth. The high surface area/roughness implant texture grew significantly more bacteria at 24 hours, whereas the minimal surface area/roughness implant textures grew significantly fewer bacteria of all types at 24 hours. For implants with intermediate and low surface areas, some species differences were observed, indicating possible affinity of specific bacterial species to surface morphology.
Conclusions: Implant shells should be reclassified using surface area/roughness into four categories (high, intermediate, low, and minimal). This classification is superior to the use of descriptive terms such as macrotexture, microtexture, and nanotexture, which are not well correlated with objective measurement and/or functional outcomes. (*Plast. Reconstr. Surg.* 142: 837, 2018.)

The texturization of the outer shell of breast implants was first introduced in 1968 with the "natural Y" implant, which incorporated a 1.2- to 2-mm polyurethane foam coating on its outer surface.[1] It was proposed that this surface prevented organized alignment of myofibroblasts, reducing the risk of capsular contracture.[1] In 1991, a specific association between polyurethane and the carcinogen 2,4-toluenediamine was reported.[2,3] This led to a voluntary withdrawal of polyurethane-coated silicone implants in the United States, which is still in place. Alternative surface technologies to modify the outer silicone

From the Surgical Infection Research Group, Faculty of Medical and Health Sciences, Macquarie University; Integrated Specialist Healthcare Education and Research Foundation; Monash University; Australian Center for Microscopy and Microanalysis, University of Sydney; and the University of Texas Southwestern.
Received for publication December 28, 2017; accepted March 30, 2018.

DOI: 10.1097/PRS.0000000000004801

Disclosure: *Professor Deva is research coordinator and consultant to Allergan, Mentor (Johnson & Johnson), Sientra, Motiva, and Acelity. Associate Professor Vickery is research coordinator and consultant to Allergan, Mentor (Johnson & Johnson), and Acelity.*

Supplemental digital content is available for this article. Direct URL citations appear in the text; simply type the URL address into any Web browser to access this content. Clickable links to the material are provided in the HTML text of this article on the *Journal*'s website (www.PRSJournal.com).

shell were introduced in an attempt to mimic the polyurethane surface. There are four processes for generating surface texture on the external silicone shell: salt loss, vulcanisation, imprinting techniques,[4] and a more recently released surface that claims a novel "nano" texture that remains proprietary.[5]

The benefits of textured implants in reducing capsular contracture remain controversial. Systematic reviews of comparative clinical studies concluded that texturization may reduce the incidence of early capsular contracture in subglandular augmentation.[6,7] Many published reports lack adequate description of implant type, surgical technique, and outcome assessment. Smaller comparative or split breast studies are evenly divided as to the benefit of texturization.[8–18]

Previous published data have confirmed that textured implants are able to support higher rates of bacterial growth in vitro.[19] Furthermore, there is a correlation between higher bacterial contamination and host response in vivo, which suggests a threshold phenomenon where bacterial load triggers a host inflammatory response.[20] More recently, bacterial infection has been proposed as one of four factors that may play a role in the genesis of breast implant–associated anaplastic large cell lymphoma (ALCL).[21] This study aimed to look at textures of varying morphology to study the relationship among surface area, roughness, and capacity for bacterial attachment and growth in vitro.

MATERIALS AND METHODS

Implant Surfaces Tested

Eleven implant surface types were subjected to testing: Silimed polyurethane (Sientra, Dallas, Texas); Polytech POLYtxt (Polytech Health and Aesthetics, Dieburg, Germany); Mentor Siltex and Mentor Smooth (Mentor Worldwide LLC, Irvine, Calif.); Motiva SilkSurface and Motiva VelvetSurface (Motiva Alajuela, Costa Rica); Allergan Biocell (Allergan, Dublin, Ireland); Allergan Natrelle Smooth (Allergan); Nagor Nagotex (Nagor Ltd, Glasgow, UK); Sientra Smooth (Santa Barbara, Calif.); and Eurosilicone textured (Eurosilicone, Apt Cedex, France). Table 1 lists the manufacturing types for the various textured surfaces.

Table 1. Manufacturing Process for Textured Implants

Manufacturing Type	Implant Type
Polyurethane bonded foam	Silimed polyurethane
Salt loss	Allergan Biocell
	Eurosilicone texture
	Nagor Nagotex
Vulcanisation (ammonium carbonate)	Polytech POLYtxt
Imprinting	Mentor Siltex
Unknown	Motiva VelvetSurface
	Motiva SilkSurface

Implant Surface Imaging

Scanning Electron Microscopy

Following fixation in 3% glutaraldehyde, samples (up to 1 cm^2) were dehydrated in ethanol and immersed in hexamethyldisilazane (Polysciences, Inc., Warrington, Pa.) for 3 minutes, and the hexamethyldisilazane was allowed to evaporate overnight. Samples were mounted onto aluminium stubs (ProSciTech, Thuringowa, Queensland, Australia) and sputter-coated with 20-nm gold film in the Emitech K550 gold coater (Emitech, West Sussex, United Kingdom). The gold-coated breast implant samples were visualized using a JEOL 6480LA scanning electron microscope (JEOL Ltd., Tokyo, Japan).

Micro–Computed Tomographic Scan

The specimens were mounted horizontally on a metal pin with adhesive before loading into a pin vice holder. These were then scanned in a Zeiss Xradia MicroXCT-400 system operating in absorption mode with a peak source energy of 50 kV and a beam current of 200 μA (Carl Zeiss, Oberkochen, Germany). The projections were collected every 0.25 degree over a total rotation of 180 degrees, with an exposure time of 3 seconds and saved as 16-bit images in a proprietary file format.

The projections were reconstructed using XMReconstructor v7.0.2817 (Zeiss Xradia) with consistent reconstruction parameters, resulting in 2.2-μm isotropic voxels. Surface area and roughness measurements were taken from this model to calculate the various required material properties. Analysis was performed with Avizo 9.3 (FEI Visualization Sciences Group, Bordeaux, France) and Fiji,[22] where a binarized model of the sample was produced by thresholding after noise-reduction filtering of the reconstructed slices.

Surface Area Determination

The three-dimensional–to–two-dimensional sample size surface area ratio was calculated by first measuring the surface area of the interface between the binarized sample and air (SA_{3D}) and then comparing it to the x-y dimensions of the sample itself (SA_{2D}). (**See Figure, Supplemental**

Digital Content 1, which shows the algorithm for calculation of the three-dimensional–to–two-dimensional area ratio, ***http://links.lww.com/PRS/C956***.). All ratios were normalized to smooth implants.

Surface Roughness Determination

To measure the roughness of the surface of each sample, it was necessary to first wrap the sample to avoid overhangs and cavities. To simplify things, a new surface was created by effectively dropping an thin probe toward the surface at each point. At the point of contact with the sample, the new surface was defined. The arithmetic mean deviation of the assessed profile (S_a) was calculated over this approximated surface by means of the following:

$$S_a = \frac{1}{kn}\sum_{j=1}^{k}\sum_{i=1}^{n}\left|y_{ij} - \bar{y}\right|$$

where i and j represent column and row positions, y_{ij} is the surface height at ij, and $\bar{y}$ is the mean surface height across the surface. The roughness was expressed as a multiple of the value for smooth implants.

In Vitro Bacterial Attachment Assay

In vitro analysis was conducted on nine types of implants of varying morphology, against four bacterial types: *Staphylococcus epidermidis*, *S. aureus*, *Pseudomonas aeruginosa*, and *Ralstonia pickettii*. The implants were prepared by cutting a strip of implant shell from the whole implant and scraping away any residual silicone from the inner surface with the blunt edge of a knife. Sections of the implant shell were obtained using a 5-mm punch biopsy tool. The implants sections were placed outside surface down in a glass petri dish and sterilized under dry heat conditions at 115°C for 39 hours. After sterilization, sterile water was added to each petri dish and the implants were pressed into the water and the air was expelled. Then, 10% tryptone soy broth containing 10^5 cells/ml of *S. epidermidis*, *S. aureus*, and *R. pickettii* or 10^4 cells/ml of *P. aeruginosa* was added to the petri dish and the implants were incubated at 37°C for up to 24 hours.

Implant samples were removed at 2, 6, and 24 hours for *S. epidermidis* and at 24 hours for *S. aureus*, *P. aeruginosa*, and *R. pickettii* for colony-forming unit determination. The implant samples were washed three times in phosphate-buffered saline. Four implant disks were placed in 0.5 ml of phosphate-buffered saline and subjected to sonication for 20 minutes followed by 1 minute of vortexing as described previously.[19] Quantitative numbers of bacteria attached to the implant outer surface were determined by serial 10-fold dilutions and standard plate culture. Each condition was tested five times.

Statistical Analysis

Statistical analysis was conducted using the statistical package Sigma Plot 13 (Systat Software, Inc., San Jose, Calif.). For comparing different implant surfaces and bacterial attachment, the data were transformed and a one-way repeated measures analysis of variance was applied, and all pairwise multiple comparison procedures were performed using the Holm-Sidak method. If data were not distributed normally, the Kruskal-Wallis one-way analysis of variance on ranks test was performed, and all pairwise multiple comparison procedures were conducted using the Dunn method. The relationship between implant three-dimensional–to–two dimensional surface area ratio and number of attached bacteria at 24 hours was tested using Pearson correlation if distributed normally or Spearman rank order correlation if distributed nonnormally. A value of $p < 0.05$ was set as significantly different.

RESULTS

Scanning Electron Microscopy

Figure 1 demonstrates the surface morphology of some of the implants studied, demonstrating a range of appearance from highly complex with many hidden surfaces to relatively featureless.

Surface Area Determination

Analysis using fine-cut computed tomographic scans and confocal microscopy allowed visualization and calculation of surface area for each of the implant shells. Table 2 summarizes the findings. Figure 2 shows three-dimensional surface area images, which were used for calculating the three-dimensional–to–two-dimensional ratios for three of the implant surfaces. (**See Figure, Supplemental Digital Content 2**, which shows the polyurethane three-dimensional extraction, ***http://links.lww.com/PRS/C957***. **See Figure, Supplemental Digital Content 3**, which shows the polyurethane three-dimensional gray-scale reconstruction, ***http://links.lww.com/PRS/C958***. **See Figure, Supplemental Digital**

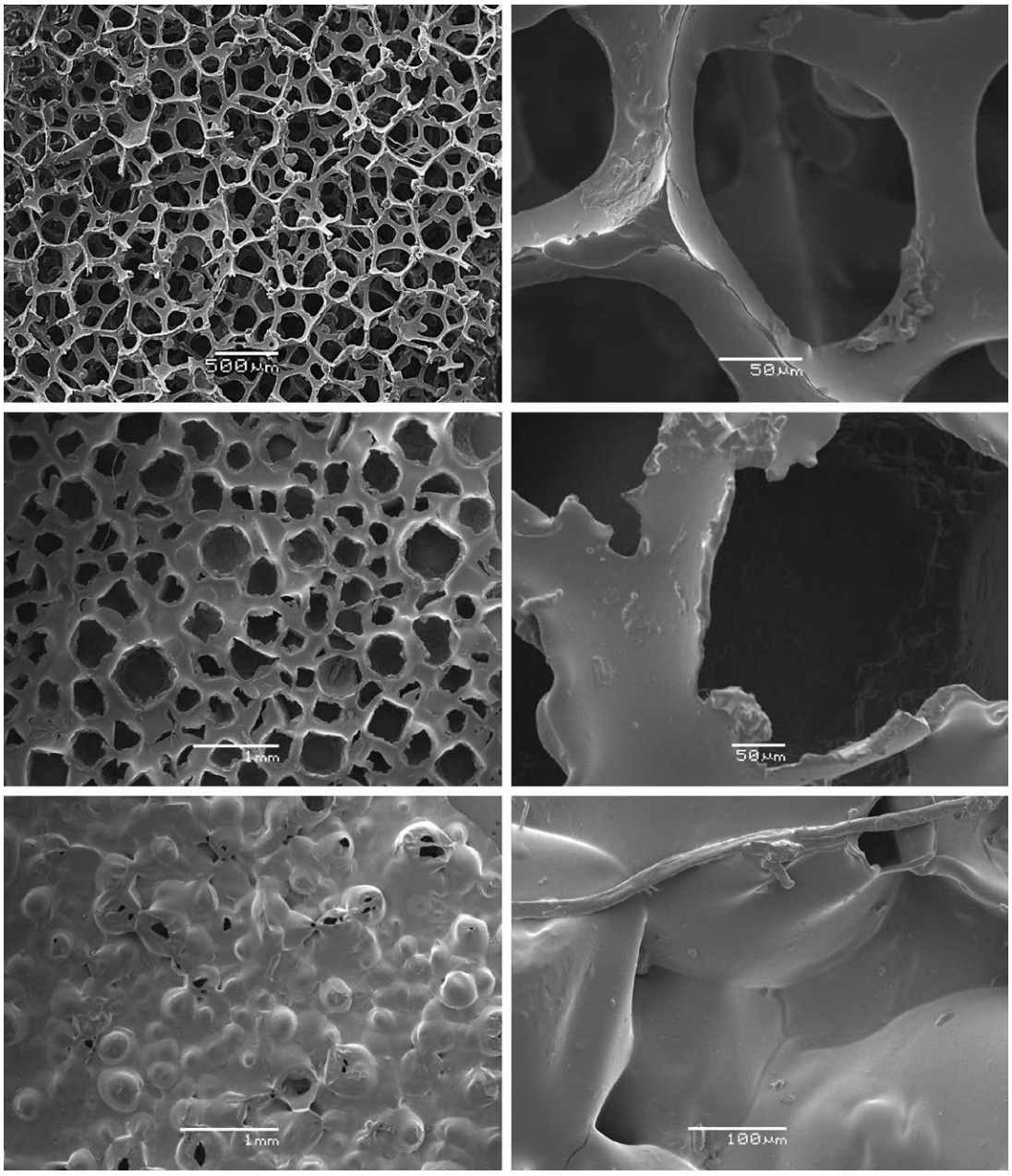

Fig. 1. Scanning electron micrographs of the surface morphology of implants studied at 25× and 400× magnification. (*Above*) Silimed polyurethane. (*Center*) Eurosilicone. (*Below*) Polytech POLYtxt.

Content 4, which shows the Polytech POLYtxt three-dimensional extraction, ***http://links.lww.com/PRS/C959***. **See Figure, Supplemental Digital Content 5**, which shows the Polytech POLYtxt three-dimensional gray-scale reconstruction, ***http://links.lww.com/PRS/C960***.) Figure 3 is a graphic representation of three-dimensional–to–two-dimensional surface area ratio.

There were four groupings for surface area measurements according to three-dimensional–to–two-dimensional surface area ratio. These were as follows: (1) high (>5), (2) intermediate (between 3 and 5), (3) low (between 2 and 3), and (4) minimal (<2).

These categories corresponded generally to implant shell manufacturing processes, with polyurethane open pore having the highest surface area; some salt-loss type and vulcanisation as intermediate; other salt-loss and imprinting type textures as low; and smooth and "nano" labeled surfaces as minimal. Salt-loss textures may vary in surface area dependent on the size of the crystals selected in the process. Interestingly, although the Polytech POLYtxt had a high surface area

Table 2. Raw Surface Area Calculation and Three-Dimensional–to–Two-Dimensional Surface Area Ratio for Each Implant Type

Implant Type	3D Surface Area (from 1.4 × 1.4-mm square) (mm^2)	3D-to-2D Surface Area Ratio*
Silimed polyurethane	79	20.8
Eurosilicone textured	15	3.9
Allergan Biocell	12	3.2
Polytech POLYtxt†	12	3.2
Nagor Nagotex	10	2.8
Mentor Siltex	8.1	2.2
Motiva VelvetSurface	4.3	1.2
Sientra Smooth	4.1	1.1
Motiva SilkSurface	3.9	1.1
Allergan Smooth	3.9	1.0
Mentor Smooth	3.8	1.0

3D, three-dimensional; 2D, two-dimensional.
*Normalized to Mentor Smooth.
†Represents available surface area after exclusion of internal cavities.

reading on first analysis, many of these surfaces were contained within the structure of the silicone outer shell and had no direct communication to the outer surface. An analysis of the choke zones (variation between 1 and 10 μm and hidden "caves" of sequestered internal surfaces) allowed an available surface area to be determined using subtractive analysis. The three-dimensional–to–two-dimensional surface area ratio for Polytech POLYtxt was calculated assuming a mean choke size of 5 μm. [**See Figure, Supplemental Digital Content 6**, which shows the demonstration of caves (sequestered surface area) for Polytech POLYtxt colored red on three-dimensional reconstruction, ***http://links.lww.com/PRS/C961***. **See Video, Supplemental Digital Content 7**, which shows real-time demonstration of caves (sequestered surface area) for Polytech POLYtxt colored red on three-dimensional reconstruction, ***http://links.lww.com/PRS/C962***.]

Surface Roughness Determination

There were four groupings for surface roughness measurements. These were as follows: (1) high (>150), (2) intermediate (between 75 and 150), (3) low (between 25 and 75), and (4) minimal (<25). Table 3 and Figure 4 summarize surface roughness findings.

In Vitro Bacterial Attachment Assay

S. epidermidis

Figure 5 shows the number of *S. epidermidis* attached to different types of implant outer shells at 2, 6, and 24 hours. Even by the 2-hour time point, the high surface area of textured Silimed polyurethane implants had a significantly larger number of bacteria attached to them than less textured implants with lower surface areas such as Mentor Siltex, smooth (i.e., Mentor, Sientra, and Allergan), Motiva VelvetSurface, and Motiva SilkSurface ($p < 0.001$). By 24 hours, implants with high or intermediate three-dimensional–to–two-dimensional surface area ratios had significantly more bacteria attached to them than implants with low or minimal three-dimensional–to–two-dimensional surface area ratios ($p < 0.001$), and although Silimed polyurethane implants had more bacteria attached to them, this was not significantly different from implants with intermediate profiles (Fig. 6, *above*). Within the salt-loss–produced implants, roughly double the number of *S. epidermidis* attached to Nagor Nagotex implants ($p < 0.4$). At 24 hours, the number of bacteria attached to the smooth implant shell was no different from the number attached to implants with a low or minimal profile ($p > 0.07$); however, it was significantly less than the number of bacteria attached to implants with intermediate to high profiles ($p < 0.001$). Over time, the number of bacteria attached to implants was positively correlated with the three-dimensional–to–two-dimensional surface area ratio; the higher the three-dimensional–to–two-dimensional surface area ratio, the more bacteria that were attached ($R = 0.64$; $p < 0.001$).

S. aureus

Figure 6, *below*, shows the number of *S. aureus* attached to different types of silicone implant outer shells at 24 hours. Silimed polyurethane implants had significantly more bacteria attached to them than any other implant ($p < 0.05$), whereas smooth implants (i.e., Mentor, Sientra, and Allergan) had significantly fewer bacteria attached to them than any other implant ($p < 0.001$) except Mentor Siltex ($p = 0.4$). There was no significant difference in the number of bacteria that attached to the three salt-loss implants. The number of bacteria attached to implants was positively correlated with the three-dimensional–to–two-dimensional surface area ratio; the higher the three-dimensional–to–two-dimensional surface area ratio, the more bacteria that were attached ($R = 0.75$; $p < 0.001$).

P. aeruginosa

Figure 7, *above*, shows the number of *P. aeruginosa* attached to differing implant shells at 24 hours. The maximum number of bacteria attached to Silimed polyurethane implants, followed by Polytech POLYtxt, and the Biocell implant produced by salt loss. The other two salt-loss implants, Eurosilicone textured and Nagor Nagotex, had

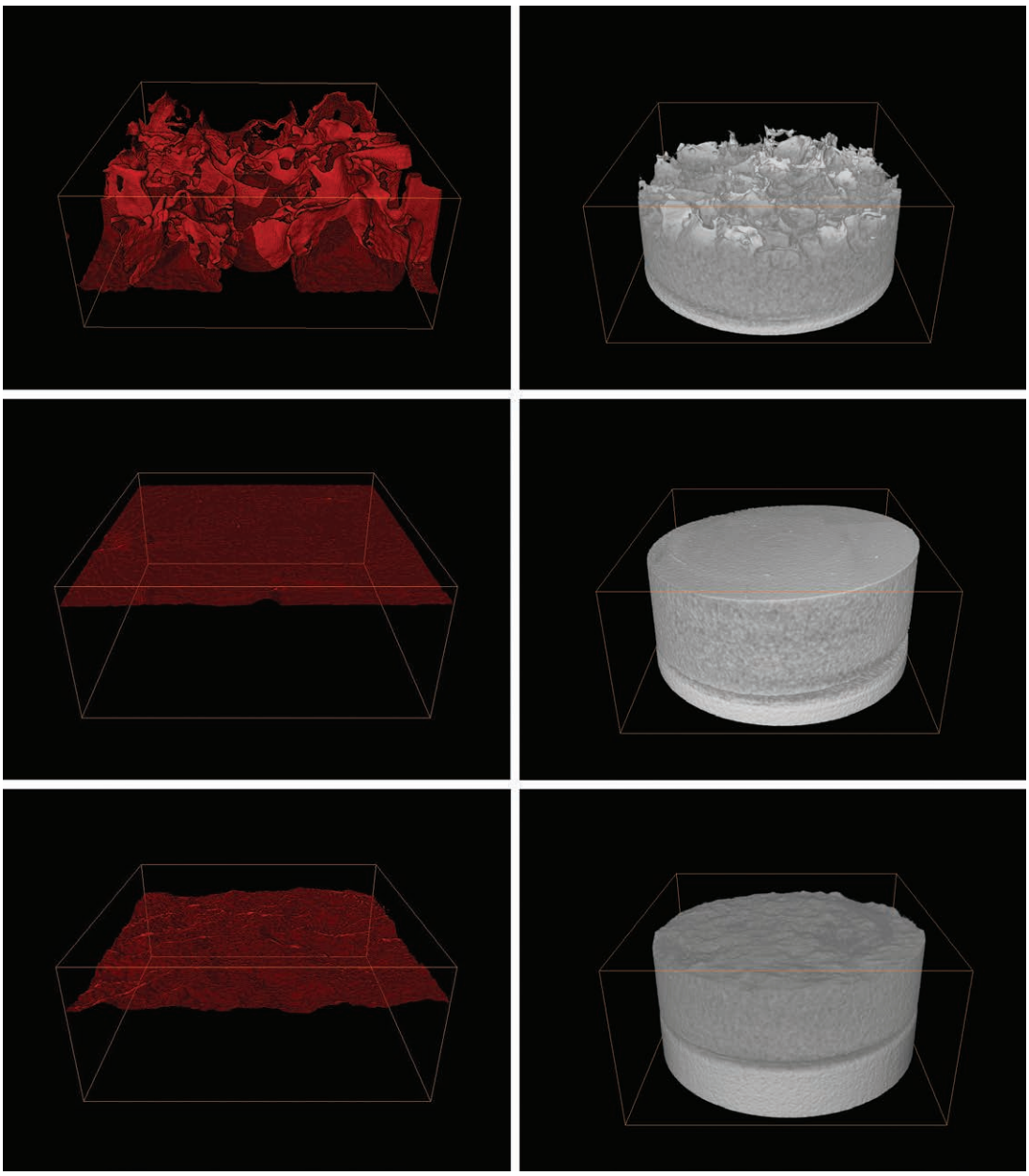

Fig. 2. Samples of three-dimensional cross-sections: extraction (*left*), and gray-scale reconstruction (*right*) from micro–computed tomographic analysis used for measurement of surface area/roughness. (*Above*) Allergan Biocell. (*Center*) Mentor Smooth. (*Below*) Motiva VelvetSurface.

less bacteria attached at 24 hours, but this was not significantly different from the numbers attached to the Biocell implant ($p > 0.09$). The number of bacteria attached to implants was positively correlated with the three-dimensional–to–two-dimensional surface area ratio; the higher the three-dimensional–to–two-dimensional surface area ratio, the more bacteria that were attached ($R = 0.81$; $p < 0.001$). Significantly fewer bacteria grew on smooth implants compared with all other implants ($p < 0.001$). In contrast to the findings for staphylococcal species, significantly fewer bacteria attached to Motiva VelvetSurface implants compared with Motiva SilkSurface implants ($p = 0.008$); the number was significantly less than for all of the other implants ($p < 0.001$).

R. pickettii

Figure 7, *below*, shows the number of *R. pickettii* attached to the different types of silicone outer shell at 24 hours. Only Silimed polyurethane, Biocell, and Nagor Nagotex had significantly more bacteria attached than smooth implants

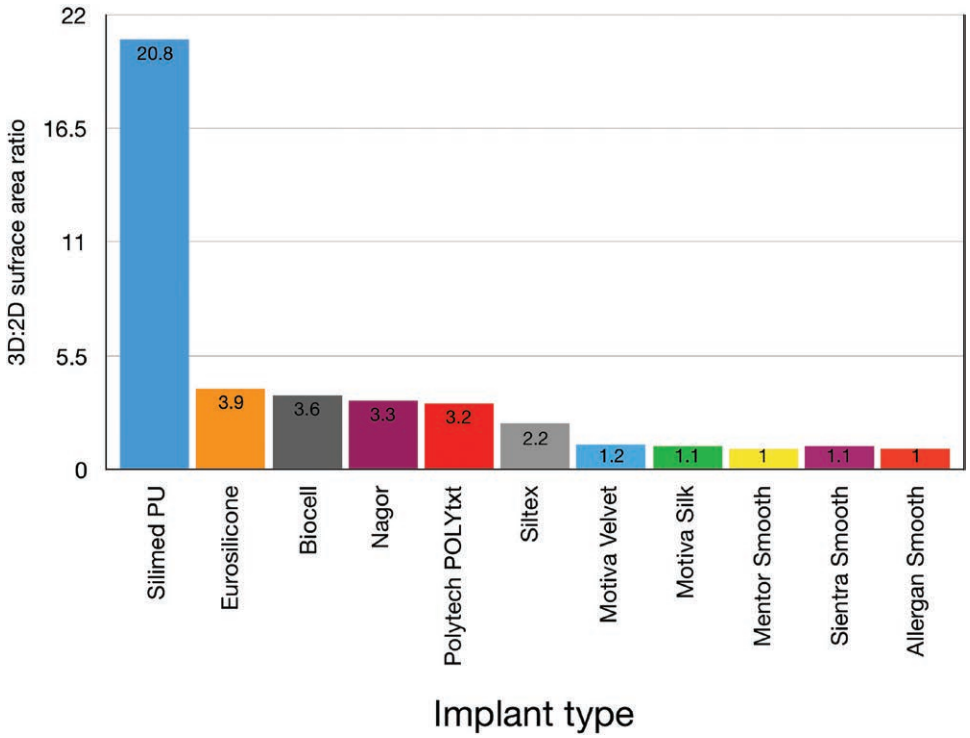

Fig. 3. Three-dimensional–to–two-dimensional surface area ratios (*3D:2D*) for various implant types studied. *PU*, polyurethane.

($p < 0.001$). There was no significant difference in the number of bacteria attached to the three salt-loss–produced implants. The number of bacteria attached to implants was positively correlated with the three-dimensional–to–two-dimensional surface area ratio; the higher the three-dimensional–to–two-dimensional surface area ratio, the more bacteria that were attached ($R = 0.87$; $p < 0.001$).

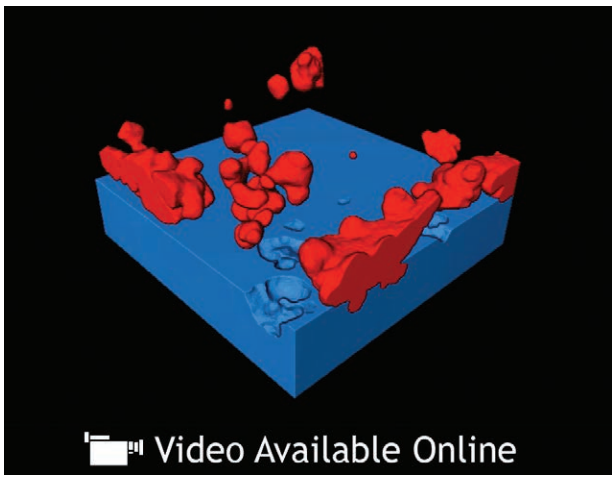

Video. Supplemental Digital Content 7 shows real-time demonstration of caves (sequestered surface area) for Polytech POLYtxt colored red on three-dimensional reconstruction, ***http://links.lww.com/PRS/C962***.

Combined Categories

Figure 8 summarizes the proposed surface classification based on combining surface area with surface roughness. The surface grade can then be combined with a nomenclature to define fill, surface, shape, and size of the implant. Table 4 summarizes the proposed classification. A Cohesive Gel 410 Allergan Biocell Anatomic 330-cc implant, for example, would be classified as GF4A330.

DISCUSSION

These findings support the use of a new classification system for implant outer shells based on measurable parameters of surface area and

Table 3. Surface Roughness for Each Implant Type

Implant Type	Surface Roughness	SD
Silimed polyurethane	277.6	32.5
Eurosilicone textured	111.7	24.9
Allergan Biocell	91.7	13.9
Nagor Nagotex	60.9	12.3
Polytech POLYtxt	58.8	19.2
Mentor Siltex	51.4	12.1
Motiva VelvetSurface	12.9	1.7
Motiva SilkSurface	20.1	0.3
Allergan Smooth	8.5	1.4
Sientra Smooth	8.1	0.8
Mentor Smooth	2.1	0.9

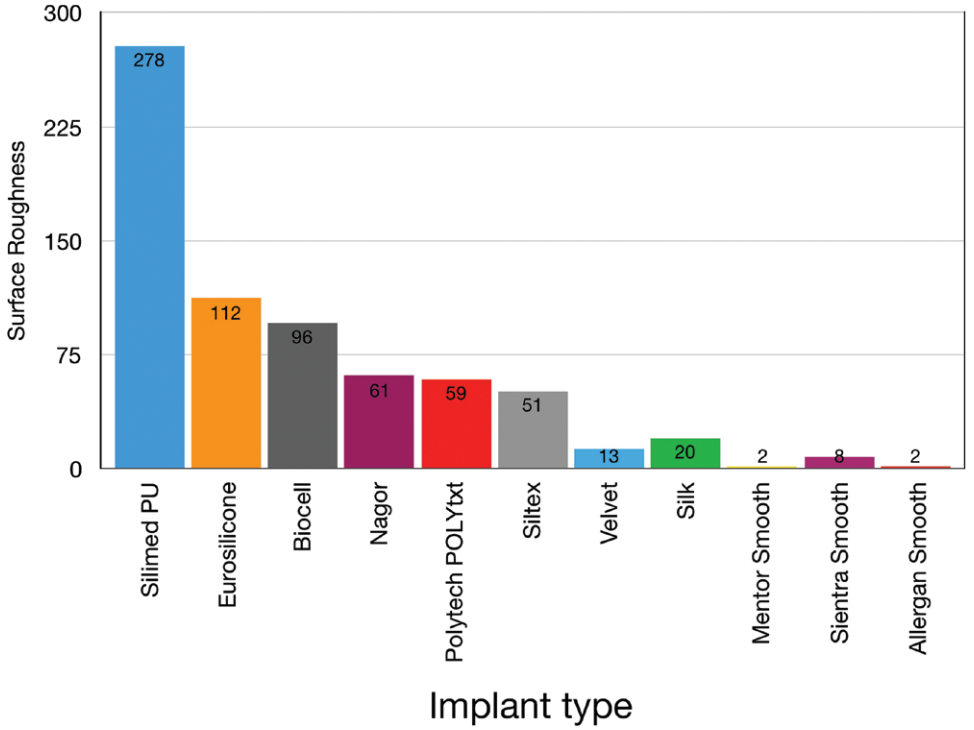

Fig. 4. Surface roughness for various implants studied. *PU*, polyurethane; *error bars* = SD.

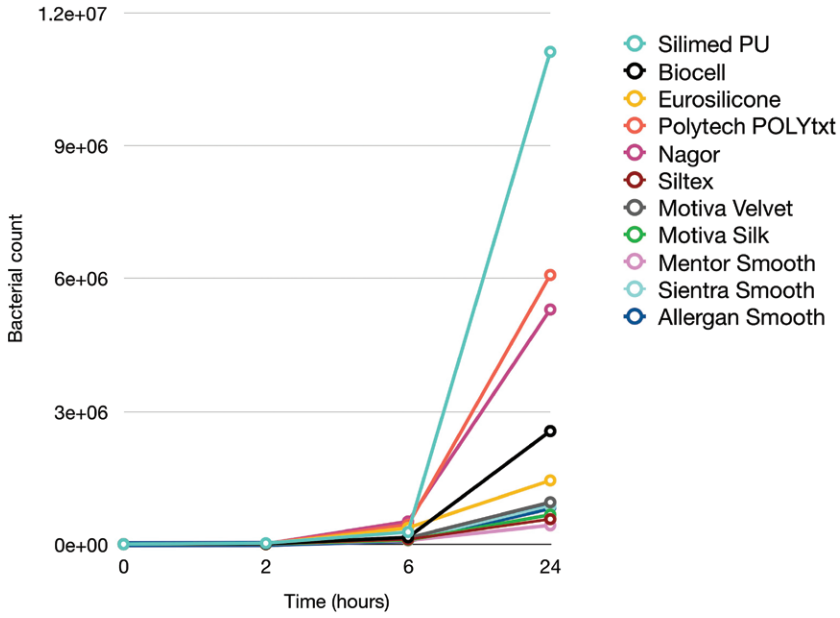

Fig. 5. *S. epidermidis* attachment and growth on various implants shells measured at 0, 2, 6, and 24 hours.

roughness that correlate with bacterial growth. We now propose a classification of implant surfaces into four grades (high, intermediate, low, and minimal) based on the direct measurement of their surface area and roughness.

Analysis of bacterial growth over varying implant surfaces showed a significant correlation, with the three-dimensional–to–two-dimensional surface area ratio demonstrating a linear relationship of bacterial attachment and growth as the surface area ratio increased. Figure 5 confirms the exponential growth rates for higher surface area textured implants for *S. epidermidis* we have reported previously.[19] The Silimed polyurethane

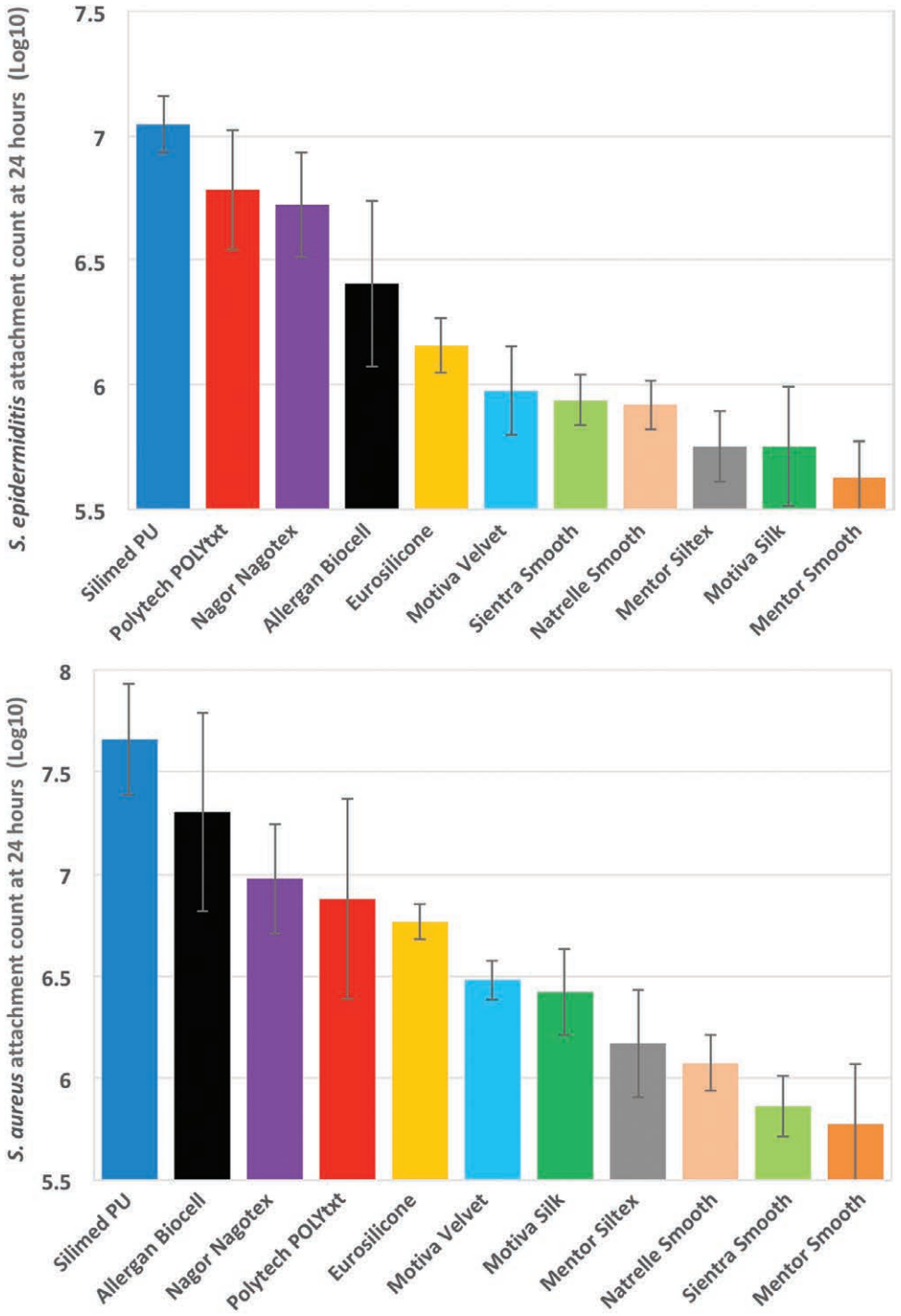

Fig. 6. Twenty-four–hour attachment and growth of bacteria on various implant shells. (*Above*) *S. epidermidis* attachment and growth on various implant shells measured at 24 hours. (*Below*) *S. aureus* attachment and growth on various implant shells measured at 24 hours. *PU*, polyurethane.

texture grew significantly higher numbers of bacteria for all species at 24 hours. Interestingly, the intermediate-surface-area implants showed good correlation and were no different from the high-surface-area implants for *S. epidermidis* and *P. aeruginosa*. These prolific biofilm formers may well overwhelm the surface area available and reach maximal growth capacity earlier than other species. These species and surface differences for intermediate/low texture require further investigation and may relate to the available surface area, specific bacterial cell size, motility, and capacity to

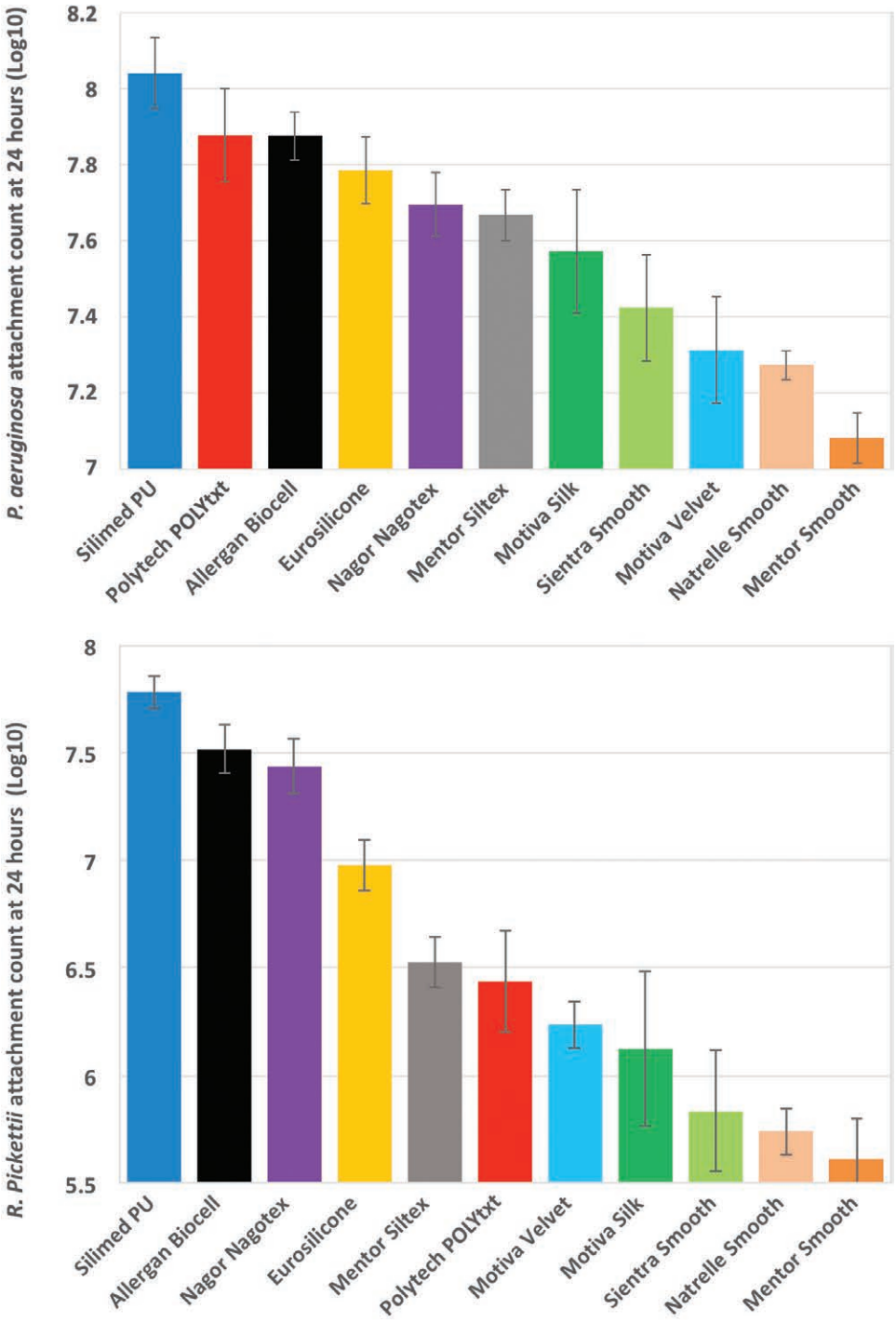

Fig. 7. Twenty-four–hour attachment and growth of bacteria on various implant shells. (*Above*) *P. aeruginosa* attachment and growth on various implant shells measured at 24 hours. (*Below*) *R. pickettii* attachment and growth on various implant shells measured at 24 hours. *PU*, polyurethane.

form biofilm together with environmental factors and availability of nutrition.

The Polytech POLYtxt surface showed a high proportion of hidden surface area (caves) within the substance of the texture. These were either walled off entirely from the external environment or had very narrow choke zones to reduce the passage of bacteria and/or host cells. This may also explain higher growth for some species for this texture. Atlan et al.[23] have used similar measurement techniques and demonstrated variation in texture morphology on different sites of the same

Process	Polyurethane foam	Salt Loss (Biocell/ Eurosilicone)	Vulcanisation	Salt Loss (Nagotex)	Imprinting	Smooth/Nano
Surface Area	High	Intermediate	Intermediate	Low	Low	Minimal
Roughness	High	Intermediate	Low	Low	Low	Minimal
SURFACE TYPE	4	3	3	2	2	1

Fig. 8. Implant surface classification relating manufacturing method, surface area, and surface roughness.

implant. This was beyond the scope of this study but will be the subject of future bacterial attachment analysis.

Previously published morphologic analyses of breast implant outer shells have used confocal microscopy,[24–26] scanning electron microscopy,[25] and/or light microscopy[26] and wettability[25] to classify implant surfaces. We have previously used these techniques[21] but found significant errors when examining higher thickness implant textures with loss of resolution in deeper zones. The use of the micro–computed tomography method has allowed a more accurate morphologic assessment of the entire implant shell. These authors have also used fibroblast adhesion and/or macrophage activation as surrogate markers for predictors of tissue incorporation and reduction in capsular contracture.[25] Although these in vitro factors may be important, they have yet to translate into proven clinical benefit; thus, their functional significance will need to be validated by clinical studies.

Table 4. Proposed Generic Breast Implant Classification Based on Fill, Surface, Shape, and Size

Characteristic	Definition
Fill	
GF	Gel filled
S	Saline filled
A	Part air filled
Surface area	
4	High
3	Intermediate
2	Low
1	Minimal
Shape	
A	Anatomical
R	Round
Size	In cubic centimeters (cc)

The presence of bacteria, by contrast, on the surface of implants has been shown to be a significant potentiator for the formation of capsular contracture in clinical and laboratory studies.[19,27,28] Clinical correlation has confirmed a significant correlation of bacterial contamination with increasing grade of capsular contracture.[29] In patients with high-grade capsular contracture, polyurethane texture was also shown to support a significantly higher load of bacteria compared with other textured implants.[20] Furthermore, translational research has now supported the use of antibacterial mitigation to reduce capsular contracture, thus linking the surface area/bacterial growth relationship directly to a functional clinical outcome.[30,31]

We are not claiming that textured implants cause more contracture, as is often suggested in commentaries critiquing our previous findings. Surface texture provides a dual opportunity for

better host tissue incorporation but also, unfortunately, for bacterial growth and proliferation. In the event that bacterial contamination is kept low, the advantages of a textured surface may well promote better long-term results. High-quality clinical comparative studies are still required to confirm this finding. It is also likely that factors other than implant texture alone have a suppressive effect on the development of biofilm and subsequent capsular contracture, including antibacterial pocket irrigation, prophylactic antibiotic use, avoidance of contamination, anatomical pocket location, and careful atraumatic dissection of the breast pocket.[27,32] Strategies to prevent contamination of the implant as it is placed help to reduce the numbers of bacteria and keep the contamination below threshold.[33] This underscores the importance of overall bacterial load on breast implants that ultimately drives the clinical outcome.

More recently, an antigen driver for breast implant–associated ALCL has been proposed. This along with surface texture, patient genetics, and time form the unifying hypothesis that explains both observed biology and epidemiology of breast implant–associated ALCL.[21] The propensity for high- and intermediate-surface-area textured implants to cause breast implant–associated ALCL is 10 times higher than for low-surface-area texture and is consistent with these data.[21] The need for a biological antigen to drive carcinogenesis indicates that it is likely that bacterial proteins rather than inert silicone particles initiate the stimulation and transformation of T cells.[34] The pathway from bacterial antigen stimulation to lymphoma has been proven for *Helicobacter pylori*, gastric mucosa-associated lymphoid tissue lymphoma, and gastric cancer.[35] Understanding the interaction among genes, the microbiome, and immunity may well provide new approaches to both the treatment and prevention of cancer.

CONCLUSIONS

We support the use of a novel and functional classification of implant outer shells based on objective measurement into four degrees of surface texture: high, intermediate, low, and minimal. The correlation of surface area/roughness with propensity for bacterial growth links this classification to a functional outcome and strengthens its validity as a tool to help surgeons to select the optimal implant surface for both breast augmentation and reconstruction.

Anand K. Deva, B.Sc.(Med.), M.B.B.S., M.S.
Suite 301, 2 Technology Place
Macquarie Park, New South Wales 2109, Australia
anand.deva@mq.edu.au

ACKNOWLEDGMENTS

The authors acknowledge the facilities and the scientific and technical assistance of the Australian Microscopy & Microanalysis Research Facility at the Australian Centre for Microscopy & Microanalysis at the University of Sydney. The authors would like to thank implant manufacturers for supply of sample implant surfaces for the study.

REFERENCES

1. Ashley FL. Further studies on the natural-Y breast prosthesis. *Plast Reconstr Surg.* 1972;49:414–419.
2. Chan SC, Birdsell DC, Gradeen CY. Urinary excretion of free toluenediamines in a patient with polyurethane-covered breast implants. *Clin Chem.* 1991;37:2143–2145.
3. Chan SC, Birdsell DC, Gradeen CY. Detection of toluenediamines in the urine of a patient with polyurethane-covered breast implants. *Clin Chem.* 1991;37:756–758.
4. Henderson PW, Nash D, Laskowski M, Grant RT. Objective comparison of commercially available breast implant devices. *Aesthetic Plast Surg.* 2015;39:724–732.
5. Sforza M, Zaccheddu R, Alleruzzo A, et al. Preliminary 3-year evaluation of experience with SilkSurface and VelvetSurface Motiva silicone breast implants: A single-center experience with 5813 consecutive breast augmentation cases. *Aesthet Surg J.* 2018;38(Suppl 2):S62–S73.
6. Wong CH, Samuel M, Tan BK, Song C. Capsular contracture in subglandular breast augmentation with textured versus smooth breast implants: A systematic review. *Plast Reconstr Surg.* 2006;118:1224–1236.
7. Barnsley GP, Sigurdson LJ, Barnsley SE. Textured surface breast implants in the prevention of capsular contracture among breast augmentation patients: A meta-analysis of randomized controlled trials. *Plast Reconstr Surg.* 2006;117:2182–2190.
8. Fagrell D, Berggren A, Tarpila E. Capsular contracture around saline-filled fine textured and smooth mammary implants: A prospective 7.5-year follow-up. *Plast Reconstr Surg.* 2001;108:2108–2112; discussion 2113.
9. Tarpila E, Ghassemifar R, Fagrell D, Berggren A. Capsular contracture with textured versus smooth saline-filled implants for breast augmentation: A prospective clinical study. *Plast Reconstr Surg.* 1997;99:1934–1939.
10. Burkhardt BR, Eades E. The effect of Biocell texturing and povidone-iodine irrigation on capsular contracture around saline-inflatable breast implants. *Plast Reconstr Surg.* 1995;96:1317–1325.
11. Burkhardt BR, Demas CP. The effect of Siltex texturing and povidone-iodine irrigation on capsular contracture around saline inflatable breast implants. *Plast Reconstr Surg.* 1994;93:123–128; discussion 129–130.
12. Asplund O, Gylbert L, Jurell G, Ward C. Textured or smooth implants for submuscular breast augmentation: A controlled study. *Plast Reconstr Surg.* 1996;97:1200–1206.
13. Hakelius L, Ohlsén L. A clinical comparison of the tendency to capsular contracture between smooth and textured

gel-filled silicone mammary implants. *Plast Reconstr Surg.* 1992;90:247–254.
14. Collis N, Coleman D, Foo IT, Sharpe DT. Ten-year review of a prospective randomized controlled trial of textured versus smooth subglandular silicone gel breast implants. *Plast Reconstr Surg.* 2000;106:786–791.
15. Malata CM, Feldberg L, Coleman DJ, Foo IT, Sharpe DT. Textured or smooth implants for breast augmentation? Three year follow-up of a prospective randomised controlled trial. *Br J Plast Surg.* 1997;50:99–105.
16. Poeppl N, Schreml S, Lichtenegger F, Lenich A, Eisenmann-Klein M, Prantl L. Does the surface structure of implants have an impact on the formation of a capsular contracture? *Aesthetic Plast Surg.* 2007;31:133–139.
17. Coleman DJ, Foo IT, Sharpe DT. Textured or smooth implants for breast augmentation? A prospective controlled trial. *Br J Plast Surg.* 1991;44:444–448.
18. Stevens WG, Nahabedian MY, Calobrace MB, et al. Risk factor analysis for capsular contracture: A 5-year Sientra study analysis using round, smooth, and textured implants for breast augmentation. *Plast Reconstr Surg.* 2013;132:1115–1123.
19. Jacombs A, Tahir S, Hu H, et al. In vitro and in vivo investigation of the influence of implant surface on the formation of bacterial biofilm in mammary implants. *Plast Reconstr Surg.* 2014;133:471e–480e.
20. Hu H, Jacombs A, Vickery K, Merten SL, Pennington DG, Deva AK. Chronic biofilm infection in breast implants is associated with an increased T-cell lymphocytic infiltrate: Implications for breast implant-associated lymphoma. *Plast Reconstr Surg.* 2015;135:319–329.
21. Loch-Wilkinson A, Beath KJ, Knight RJW, et al. Breast implant-associated anaplastic large cell lymphoma in Australia and New Zealand: High-surface-area textured implants are associated with increased risk. *Plast Reconstr Surg.* 2017;140:645–654.
22. Schindelin J, Arganda-Carreras I, Frise E, et al. Fiji: An open-source platform for biological-image analysis. *Nat Methods* 2012;9:676–682.
23. Atlan M, Bigerelle M, Larreta-garde V, Hindié M, Hedén P. Characterization of breast implant surfaces, shapes, and biomechanics: A comparison of high cohesive anatomically shaped textured silicone, breast implants from three different manufacturers. *Aesthetic Plast Surg.* 2016;40:89–97.
24. Valencia-Lazcano AA, Alonso-Rasgado T, Bayat A. Characterisation of breast implant surfaces and correlation with fibroblast adhesion. *J Mech Behav Biomed Mater.* 2013;21:133–148.
25. Barr S, Hill EW, Bayat A. Functional biocompatibility testing of silicone breast implants and a novel classification system based on surface roughness. *J Mech Behav Biomed Mater.* 2017;75:75–81.
26. Barr S, Hill E, Bayat A. Current implant surface technology: An examination of their nanostructure and their influence on fibroblast alignment and biocompatibility. *Eplasty* 2009;9:e22.
27. Chong SJ, Deva AK. Understanding the etiology and prevention of capsular contracture: Translating science into practice. *Clin Plast Surg.* 2015;42:427–436.
28. Rieger UM, Mesina J, Kalbermatten DF, et al. Bacterial biofilms and capsular contracture in patients with breast implants. *Br J Surg.* 2013;100:768–774.
29. Rieger UM, Raschke GF, Frei R, Djedovic G, Pierer G, Trampuz A. Role of bacterial biofilms in patients after reconstructive and aesthetic breast implant surgery. *J Long Term Eff Med Implants* 2014;24:131–138.
30. Blount AL, Martin MD, Lineberry KD, Kettaneh N, Alfonso DR. Capsular contracture rate in a low-risk population after primary augmentation mammaplasty. *Aesthet Surg J.* 2013;33:516–521.
31. Giordano S, Peltoniemi H, Lilius P, Salmi A. Povidone-iodine combined with antibiotic topical irrigation to reduce capsular contracture in cosmetic breast augmentation: A comparative study. *Aesthet Surg J.* 2013;33:675–680.
32. Adams WP Jr. Capsular contracture: What is it? What causes it? How can it be prevented and managed? *Clin Plast Surg.* 2009;36:119–126, vii.
33. Deva AK, Adams WP Jr, Vickery K. The role of bacterial biofilms in device-associated infection. *Plast Reconstr Surg.* 2013;132:1319–1328.
34. Kadin ME, Deva A, Xu H, et al. Biomarkers provide clues to early events in the pathogenesis of breast implant-associated anaplastic large cell lymphoma. *Aesthet Surg J.* 2016;36:773–781.
35. Peek RM Jr, Kuipers EJ. Gained in translation: The importance of biologically relevant models of *Helicobacter pylori*-induced gastric cancer. *Gut* 2012;61:2–3.